High heat transfer chip cooling: capillary based flow boiling model and a novel experimental analysis method

G.D. Mensink[a] *, R. Betsema[a], C.M. Rops[a], R.B.J. Koldeweij[a], P.B.T.H Boerboom[a]
[a]TNO High Tech Industry

*daniel.mensink@tno.nl

Abstract. Currently, one of the main challenges for the future miniaturization of electronics is its thermal management. As the number of transistors per square centimeter increases, the generated heat fluxes will continue to increase. Forced convection air cooling has reached its limits and does no longer comply to the imposed thermal loads. Thus more complex (forced) convection liquid cooling and flow boiling cooling are explored to fulfill the heat load demands in the near future. This investigation discusses an improved microfluidic flow boiling model, and a novel experimental analysis method to obtain the flow boiling heat transfer coefficient more accurately. The cooling performance of a cooler containing the TNO microfluidic flow boiling method is measured by quantifying the chip interface temperature and the microfluidic flow boiling heat transfer coefficient. The improved microfluidic flow boiling model captures the measured trends such as the increase of heat transfer coefficient on increasing the input heat flux and its relative independence on mass flow rate. For the maximum investigated chip heat flux of 250W/cm^2 the chip interface temperature remained below 90 ^{o}C.

Keywords: Microfluidic cooling, Two-phase heat transfer, Flow boiling, Power electronics.

1. INTRODUCTION

Over the last six decades the number of transistors per square centimeter approximately has doubled every two years. This observed trend is known as Moore's law as introduced in his IEEE speech in 1975 (Moore, 1975). Currently, one of the main challenges for the future miniaturization of electronics is its thermal management. The generated heat fluxes of the electronic devices continue to increase over the years. Over the last 20 years a linear increase is observed from approximately 50W/cm^2 to almost 200w/cm^2 (Zhang *et al*, 2021), see Figure 1.

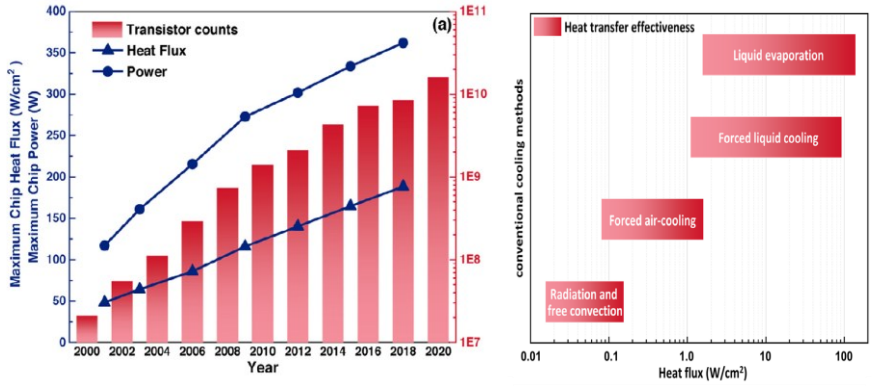

Figure 1. Left: Maximum chip power (blue dots) and maximum heat flux (blue triangles), and number of transistors per device (red bars). Right: Typical range of heat flux density of conventional cooling methods. After Zhang *et al*, 2021.

Conventional air cooling attains by itself about 0.1 W/cm^2 , see Figure 1. This number can be amplified one or two orders of magnitude by using surface enhancing techniques, and optimizing heat removal from the system (Mohammed *et al.*, 2021). However, air cooling has reached its limits. Depending on the application more efficient cooling methods are explored, such as liquid cooling, thermo-electric cooling and fluid boiling cooling.

An example of the increase in power densities can be found in the datacenter community (Rajan *et al*, 2022). Here the Thermal Design Power (TDP) in datacenters is identified to exceed 400W in 2030. Assuming the mentioned heat transferring area of about 1.5cm^2 for their investigated chips, this power corresponds to 300W/cm^2 . These numbers are similar as the projected values in the above shown heat flux and power data as given by Zhang in Figure 1. Bearing in mind the currently reported maximum cooling heat fluxes of about 100W/cm^2 , Rajan has identified two main challenges: First, the opportunity to continue unlocking the full device performance and second to contain the thermal management overhead (energy and water consumption). To address these challenges, an essential goal is to operate the devices at a

lower junction temperature (Guler *et al.*, 2020). This reduces the leakage power, and thus the energy consumption. Furthermore, a lower junction temperature increases the lifetime of the devices. Determining the junction temperature is crucial, since silicon based inverters typically allow a maximum junction temperature of about 120 ^{o}C (Kempiak *et al.*, 2018).

Another example of increasing power densities is the electrification of vehicles. During the fast charging of the battery or the operation of the electro-engine large portions of energy (300kW to 600kW) are converted from alternating to direct current or vice versa. Wide Band Gap (WBG) technologies such as SiC and GaN, increase the device's switching performance. Although the efficiency of these inverters is above 99.5% (Zhu *et al.*, 2018), the heat losses remain significant. Abramushkina *et al.* (2021) and co-workers show that these technologies can deal with maximum heat fluxes above 120W/cm^2 and elevated junction temperatures up to 175 ^{o}C.

These examples from practice show that the innovative, more efficient cooling methods are essential to attain the high heat fluxes (>100W/cm^2) and transport high amounts of thermal energy (~1kW per device). As indicated by the literature overview by Zhang *et al* (2021), two-phase cooling in microchannels is a promising solution. However, the commonly observed drawbacks of two-phase flow boiling in micro channels must be overcome such as unstable flow and intermittent reduced heat transfer (Kandlikar, 2001).

TNO has developed a microfluidic flow boiling method which ensures stable flow boiling in a microchannel structure (Rops *et al.*, 2009). Over the years TNO has refined their modelling to more accurately predict the heat transfer in these structures. Earlier it was observed that an analytical description of the lateral conduction in the heat conducting wall in their thermal models was essential for a better estimation of the chip interface temperature (Betsema *et al.*, 2022).

The current work investigates the inclusion of surface tension effects on the flow pattern to more accurately predict the microfluidic flow boiling heat transfer. In the next chapter the analytical capillary based flow boiling model for the microfluidic flow boiling structure is discussed. Next, in the third chapter, a novel experimental analysis method is proposed to estimate the microfluidic flow boiling heat transfer coefficient more accurately. Finally, the capillary based analytical model is validated using the novel experimental analysis method and conclusions are drawn.

2. CAPILLARY BASED FLOW BOILING MODEL DEVELOPMENT

Similar as reported in literature (e.g. Kandlikar, 2001, Sun *et al.*, 2018), in our microfluidic flow boiling experiments the annular flow regime is observed over a wide range of vapour qualities. Therefore, for simplicity reasons, to model the heat transfer, it is assumed that the microfluidic flow boiling takes place in an annular flow pattern. As proposed by Thome *et al.* (2004) in their so-called 3-zone model, the TNO model calculates the flow boiling heat transfer coefficient as the liquid thermal conductivity over the liquid film thickness. A thin film induces a high flow boiling heat transfer. The vapour quality in a section is dependent on the amount of energy inserted in the fluid. The void fraction, however, strongly depends on the ratio of the vapour velocity and the liquid velocity, the so-called slip velocity. Therefore the slip velocity determines the shape and thickness of the liquid film.

An accurate prediction of the film thickness is essential to model a proper flow boiling heat transfer. Thome *et al.* (2004) assume a uniform heat flux and they use a homogeneous two-phase flow model to obtain the film thickness. However, for annular flow the momentum flux model of two-phase flow is more appropriate to obtain the film thickness. Revellin *et al.* (2008) use the momentum flux model as well as an improvement to the original 3-zone model of Thome et al. (2004). Similarly, the TNO microfluidic flow boiling model, discussed in Betsema *et al.* (2022), applies a momentum approach to estimate the thickness of the liquid film. For round channels the momentum approach could yield reasonable results. However, in rectangular microchannels, such as applied in the TNO microfluidic flow boiling method, the shape of the liquid film is significantly affected by the surface tension. Typically more liquid is accumulated in the corners, therefore thinning the liquid film over the side walls. These thickness variations significantly affect the calculated heat transfer coefficient.

Wang and Rose (2005) have developed a numerical method to calculate the equilibrium state of a liquid interface in a rectangular channel. Using a dual coordinate system for the top and bottom corner a combined mass and momentum balance can be solved including viscosity, gravity and surface tension. The TNO model (Betsema, 2022) is extended with the Wang and Rose method for the film thickness calculation during evaporation. The momentum based liquid film thickness is taken as the initial shape assumption. The effect of including the surface tension on the liquid film shape is shown in Figure 2.

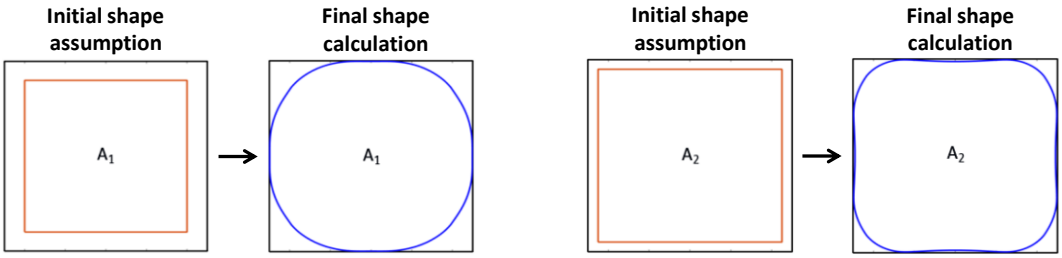

Figure 2. Surface tension effect on film shape for different void fractions, TNO microfluidic flow boiling model results. Left: void fraction 0.8. Right: void fraction 0.9.

Rops (2009) teaches that the TNO microfluidic flow boiling method consists of a staggered structure, re-distributing the liquid film to an initial shape on passing each staggering. Therefore the time evolution of the bubble shape must be taken into account. The Wang and Rose method remains a suitable approach, since their relations are essentially transient equations which they solve over a long bubble evolution time. The evolution of the bubble shape over time can be seen in the left figure of Figure 3

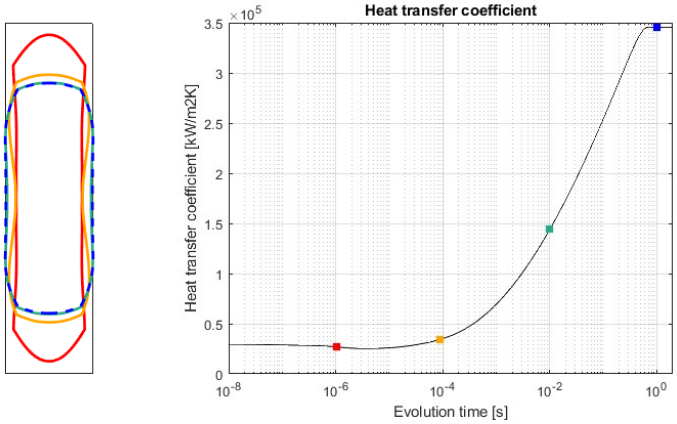

Figure 3. Left: typical evolution of bubble shape over time. Right: effect on calculated heat transfer coefficient.

Figure 3 (left) shows that the film thickness over the short horizontal walls thickens as compared to the momentum flux model. On the other hand, the liquid film over the long vertical walls thins due to the capillary forces. The overall effect on the calculated heat transfer coefficient is shown in the right graph of Figure 3. For short evolution times (eg. red marker in Figure 3) the calculated heat transfer coefficient is equal to the momentum flux model heat transfer. After approximately 0.1 millisecond the heat transfer coefficient starts to increase. Finally, for evolution times longer than 1 second the heat transfer coefficient stabilizes at roughly a factor 10 higher value than the estimate based on the initial momentum flux model film thicknesses. This clearly shows the impact of the time evolution of the film. It is should be noted that a long straight channel therefore leads to very thin films. These thin films evaporate quickly and break-up easily leading to undesired dry spots and unstable flow boiling behaviour.

3. EXPERIMENTAL ANALYSIS METHOD

Due to the typical size of a microchannel, local estimation of the temperatures and the heat fluxes is complex. Differences of about one order of magnitude are reported for experimental results at equivalent conditions although measured during different investigations (Ribatski, 2013). The unsteady flow behaviour, and the size and positioning of the temperature sensors affect the measurement (Sun *et al.*, 2018). In the early years of this millennium Zhang has performed flow boiling measurements on microchannels (Zhang, 2002). As a data reduction method and for thermal modelling, a constant heat flux is assumed. Similarly, Li and co-workers (Li *et al.*, 2017) have investigated the effect of contact angle (i.e. wettability) on micro flow boiling. In their research they use thin film heaters and local temperature sensors to estimate the local heat transfer coefficient. They assume a uniform heat flux in their analysis.

Typically in literature the average heat transfer coefficient is determined by the total heat input divided by the channel area multiplied with the estimated temperature difference between the channel wall and the fluid. Assuming a constant heat flux implies that the temperature of the liquid rises linearly to the boiling temperature. When reaching the boiling temperature it remains constant, see Figure 4.

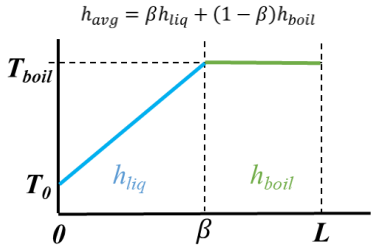

Figure 4. Schematic of fluid temperature using constant heat flux assumption.

Using this assumed temperature profile the average fluid temperature can be obtained. By means of the mass flow rate, m , heat capacity , c_p , and the constant heat flux, q'' , the boiling location, β, can be calculated:

$$\beta = \frac{x_{boil}}{L} = (T_{boil} - T_0)\frac{m \cdot c_p}{q'' \cdot w \cdot L}, \quad (1)$$

w and L are the width and the length of the channel respectively. The boiling heat transfer coefficient, h_{boil} , can be obtained from the relation for the average heat flux, h_{avg} , which is the area weighted average of the single phase liquid heat transfer coefficient, h_{liq} , and the boiling heat transfer coefficient:

$$h_{avg} = \beta h_{liq} + (1-\beta)h_{boil}. \quad (2)$$

The single phase heat transfer coefficient, h_{liq} , can be deduced from single phase only heat transfer experiments, or relations from literature can be used. By rewriting the area averaged heat transfer relation (2) and inserting equation (1), the boiling heat transfer coefficient can be obtained from the measured average heat transfer coefficient and the single phase heat transfer coefficient.

In a microchannel the wall is relatively thick compared to its length and typically the thermal conductivity of the wall material is one or two orders of magnitude larger than the thermal conductivity of the fluid. Therefore lateral conduction has a significant effect (Betsema *et al.*, 2022) on the heat distribution along the channel. Realization of a constant heat flux along the channel length is very difficult to achieve in a dedicated experiment and rather impossible for any practical implementation. At the same time, the relatively small thermal resistance in axial direction favours a constant temperature along the channel.

In practice the heat of the chip is typically spread out over a larger surface area using a heat spreader. Within this heat spreader the TNO microfluidic two-phase cooling structure can be realized, which picks up the spread heat, see the left picture of Figure 5. The current investigation applies a (near) constant wall temperature assumption as a data reduction method. In order to substantiate this assumption the heated wall of the investigated microchannel cooler is deliberately thickened. To mimic a half bridge chip cooler, an aluminium mockup setup is designed to obtain a better defined thermal boundary layer, see the right picture of Figure 5.

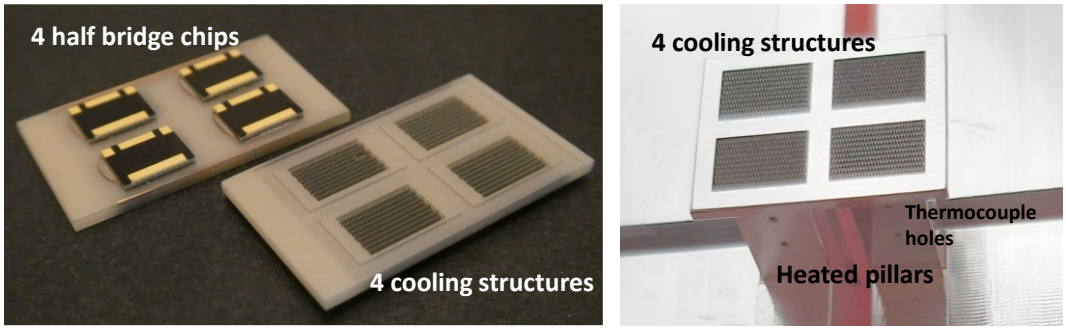

Figure 5. Left: top side with half bridge chips, and bottom side with TNO microfluidic flow boiling cooler structure. Right: Aluminum mock up setup with the pillars to mimic the chip heat load and the thermocouple holes to estimate the heat flux and wall temperature.

The aluminium pillar allows lateral heat conduction with a relatively small temperature gradient, thus approaching the uniform wall temperature at the bottom of the microfluidic flow boiling structure. By means of the two thermocouple holes above each other, the vertical temperature gradient is measured in each pillar. This vertical gradient is used to estimate the wall temperature, T_{wall} , by linear extrapolation and assuming one dimensional conduction in the pillar. The heating power supplied to the microfluidic flow boiling structure is derived as well from the vertical temperature gradient.

$$Q_{chip} = q'' \cdot A = \lambda \cdot \frac{\Delta T}{d} \cdot w \cdot L, \quad (3)$$

in which ΔT is the temperature difference between the two thermocouples placed above each other at a distance, d, and λ is the thermal conductivity of the aluminium pillar.

On assuming a constant wall temperature, the temperature of the liquid does not rise linearly to the boiling temperature. An exponential behaviour towards the wall temperature, T_{wall}, is to be expected, however cut-off at the fluid boiling temperature, T_{boil}, see Figure 6.

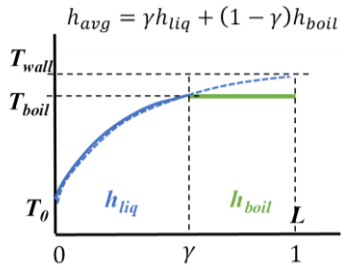

Figure 6. Schematic of fluid temperature using constant wall temperature assumption.

Again, the average heat transfer, h_{avg}, over the channel is estimated by the area weighted average of the single phase liquid heat transfer coefficient, h_{liq}, and the boiling heat transfer coefficient, h_{boil}.

$$h_{avg} = \gamma h_{liq} + (1-\gamma) h_{boil}. \quad (4)$$

However the boiling location, γ, needs to be obtained using the exponential temperature curve for the liquid, T_{liq}, as given in equation (5) and solving the position x for $T_{liq} = T_{boil}$.

$$T_{liq}(x) = T_{wall} - (T_{wall} - T_0) \cdot exp\left(-\frac{h_{liq} \cdot w}{m \cdot c_p} \cdot x\right). \quad (5)$$

This results in the following equation for the boiling location, γ:

$$\gamma = \frac{x_{boil}}{L} = \frac{m \cdot c_p}{h_{liq} \cdot w \cdot L} ln\left(\frac{T_{wall} - T_0}{T_{wall} - T_{boil}}\right), \quad (6)$$

in which w and L are the width and the length of the channel respectively, m is the mass flow rate, c_p is heat capacity of the liquid and T_{wall} is the constant wall temperature. By rewriting the area averaged heat transfer relation (4) and inserting equation (6), the boiling heat transfer coefficient can be obtained from the measured average heat transfer coefficient and the single phase heat transfer coefficient.

4. EXPERIMENTAL RESULTS AND CONCLUSIONS

The temperature at the virtual chip interface in the aluminium mock up setup and the microfluidic flow boiling heat transfer coefficient are determined for various chip powers. Figure 7 (left), shows the chip interface temperature. Even for heat fluxes up to 250W/cm^2 it remains slightly below 90 °C. The 250 W/cm^2 case corresponds to 40W per half bridge chip. Using a typical internal chip resistance of about 0.8 K/W the junction temperature remains below 120 °C at a chip dissipation of 40W. Furthermore the interface temperature is little dependent on the flow rate for a chip.

The right hand graph of Figure 7 shows the boiling heat transfer coefficient. The measured boiling heat transfer coefficient is estimated using the constant temperature assumption relations. The measured boiling heat transfer coefficient (markers) is little dependent on the flow rate. However, it must be noted that going to low flow rates, resulting in vapour qualities above 0.5 (not shown in the graph), the risk of dry-out increases. This destabilises the flow boiling process. The 250 W/cm^2 case shows the highest boiling heat transfer coefficients. This can be understood since the highest heat flux results in the thinnest liquid film.

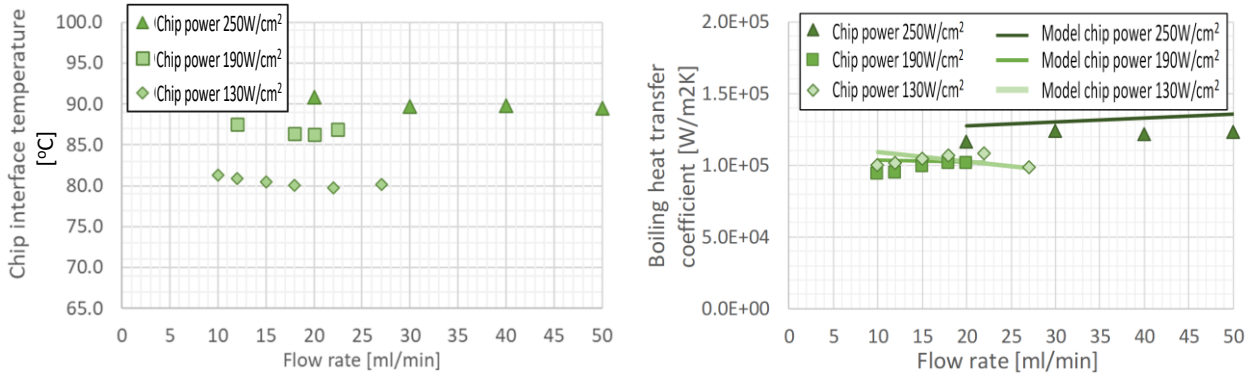

Figure 7. Microfluidic flow boiling results: experiments (markers) and model (lines). Liquid flow rates are given for one chip. Left: (virtual) chip interface temperature for three individual chip powers. Right: Estimated microfluidic flow boiling heat transfer coefficient.

The heat transfer coefficient graph (right graph of Figure 7) contains the model results with inclusion of the surface tension. A nice correspondence with the experiments is found. As shown in chapter 2, the evolution time of the film is an important parameter. The length in flow direction of the staggered boiling structure and the liquid film velocity determine the evolution time of the liquid film. The evolution time mainly depends on the heat flux and to lesser extend on the mass flow rate. Typically the evolution time increases for higher heat flux at which the liquid film thickness is less. This leads to a lower liquid velocity in the thin film. Therefore the thin films occurring at the higher heat fluxes have a longer time to evolve towards the equilibrium state. For the experiments conducted in this investigation the film evolution times are found to be in the order of 1 to 10 milliseconds.

The capillary based flow boiling model predicts the right magnitude of the flow boiling heat transfer coefficient. Next, the improved model for the heat transfer coefficient captures both the near independence on the flow rate as well as the slight increase on increasing heat flux. Therefore, the model is suited to be used as a development tool to predict the heat transfer of newly designed microfluidic flow boiling structures.

The maximum mimicked chip heat flux of 250W/cm^2 is roughly a factor 2 improvement in relation to current state-of-the-art coolers reported in literature (e.g. Zhang *et al.*, 2021). Further geometry optimisation allows to achieve cooling heat fluxes above 300W/cm^2 as foreseen for power electronics beyond 2030 (Rajan *et al.*, 2022).

5. REFERENCES

Abramushkina, E., Zhaksylyk, A., Geury, T., El Baghdadi, M., Hegazy, O., 2021, “A Thorough Review of Cooling Concepts and Thermal Management Techniques for Automotive WBG Inverters: Topology, Technology and Integration Level.”, *Energies*, vol. 14.

Betsema, R., and Rops, C.M., 2022, “A coupled model of heat spreading and flow boiling in microchannels”, *ASDAM 2022*, Smolice castle, Slovakia.

Guler, A. and Jha, N. K., 2020, “McPAT-monolithic: An area/power/timing architecture modeling framework for 3-D hybrid monolithic multicore systems,", *IEEE Trans. Very Large Scale Integr. (VLSI) Syst.*, vol. 28(10), pp. 2146-2156.

Kandlikar, S.G., 2001, “Fundamental issues related to flow boiling in minichannels and microchannels”, *Exp. Thermal and fluid science*, vol. 26., pp. 389-407.

Kempiak, C., Lindemann, A., Thal, E. and Idaka, S., 2018, "Investigation of the usage of a chip integrated sensor to determine junction temperature during power cycling tests," *10th Int. Conference on Integrated Power Electronics Systems*, Stuttgart, Germany.

Li W., Zhou K., Li J., Feng Z., and Zhu H., 2018, “Effects of heat flux, mass flux and two-phase inlet quality on flow boiling in a vertical superhydrophylic microchannel”, *International journal of Heat and Mass transfer*, vol.119, pp.601-613.

Mohammed and Razuqi, 2021, “Effect of air fan position on heat transfer performance of elliptical pin fin heat sink subjected to impinging air flow”, *Journal of thermal engineering*, vol.7(6).

Moore, G., 1975, *IEEE International Electron Devices Meeting*, Washington, D.C., USA.

Rajan, S.K., Ramakrishnan, B., Allisa, H., Kim, W., Belady, C. and Bakir, M., 2022, “Integrated silicon microfluidic cooling of a high-power overclocked CPU for efficient thermal management”, *IEEE Access Electronics packaging*, vol.10.

Revellin R., and Thome J.R., 2008, “A theoretical model for the prediction of the critical heat flux in heated microchannels”, *International Journal of Heat and Mass Transfer*, vol.51, pp.1216–1225.

Ribatski, G., 2013, “A critical overview on the recent literature concerning flow boiling and two-phase flows inside micro-scal channels”, *Experimental Heat Transfer*, vol.26, pp. 198-246.

Rops, C.M., Velthuis, J.F.M., Graaf, F. and Geers, L.F.G, 2009, “Multiple connected channel micro evaporator”, WO2009/082230.

Sun, Y., Guo, C., Jiang, Y., Wang, T. and Zhang, L., 2018, “Transient film thickness and microscale heat transfer during flow boiling in microchannels”, *International Journal of Heat and Mass Transfer*, vol.116, pp.458–470.

Thome, J.R., V. Dupont, V. and Jacobi, V., 2004, “Heat transfer model for evaporation in microchannels. Part I: presentation of the model”, *International Journal of Heat and Mass Transfer*, vol.47, pp.3375–3385.

Wang, H.S. and Rose, J.W., 2005, “Theory of film condensation in horizontal noncircular section microchannels” , *Journal of Heat Transfer*, vol. 127(10), pp.1096–1105.

Zhang L., Koo J-M., Jiang L., Asheghi M., Goodson K.E., Santiago J.G., and Kenny T.W., 2002, “*Measurements and modeling of two-phase flow in microchannels with nearly constant heat flux boundary conditions*”, Journal of microelectromechanical system, vol.11(1).

Zhang, Z., Wang, X., and Yan, Y, 2021, “A review of the state-of-the-art in electronic cooling”, *Advances in Electrical Engineering, Electronics and Energy*, Vol. 1, pp. 1-26.

Zhu, J., Kim, H., Chen, H., Erickson, R. and Maksimović, D., 2018, "High efficiency SiC traction inverter for electric vehicle applications,", *IEEE Applied Power Electronics Conference and Exposition (APEC)*, San Antonio, USA.